Motional Averaging of Nuclear Resonance in a Field Gradient

Nanette N. Jarenwattananon and Louis-S. Bouchard*
Department of Chemistry and Biochemistry, University of California Los Angeles, 607 Charles E Young Drive East, Los Angeles, California 90095-1059, USA
(Received 11 December 2014; revised manuscript received 5 March 2015; published 12 May 2015)

The traditional view of nuclear-spin decoherence in a field gradient due to molecular self-diffusion is challenged on the basis of temperature dependence of the linewidth, which demonstrates different behaviors between liquids and gases. The conventional theory predicts that in a fluid, linewidth should increase with temperature; however, in gases we observed the opposite behavior. This surprising behavior can be explained using a more detailed theoretical description of the dephasing function that accounts for position autocorrelation effects.

DOI: 10.1103/PhysRevLett.114.197601 PACS numbers: 76.60.-k, 05.20.Jj, 51.10.+y, 82.56.Lz

For over six decades, diffusion-weighted nuclear magnetic resonance (NMR) has been the flagship experiment for measurements of molecular self-diffusion in free or confined geometries. Diffusion-based NMR experiments have a wide range of applications from porous media [1], catalysis [2], materials science, and chemistry [3] to biomedicine [4]. Consider the simple experiment shown in Fig. 1, where the nuclear induction signal is read-out in the presence of a magnetic-field gradient. The gradient modulates the magnetization spatially along the gradient's direction (assuming a sufficiently strong external field so that the gradient is unidirectional). Time evolution of this magnetization in the presence of diffusion effects provides a direct and unambiguous measurement of the self-diffusion process. In the traditional description of molecular self-diffusion [5–9], a molecule undergoes a random walk whereby at each time step, the nuclear spins accumulate phase increments that are randomly drawn from a normal distribution. In the presence of a magnetic-field gradient, the decoherence of the nuclear induction signal $S(t)$ follows the well-known textbook expression [5–10]

$$S(t) = \exp\left[-(1/3)\gamma_n^2 g^2 D t^3\right], \tag{1}$$

where γ_n is the nuclear gyromagnetic ratio, D is the self-diffusion coefficient, g is the applied gradient strength, and t is time. The t^3 dependence has been extensively validated and has been utilized to measure molecular self-diffusion coefficients in a wide variety of liquids [10–12]. In a gas, however, the situation is more complicated. The assumption of a normally distributed phase accumulation at every time step is difficult to justify in light of the fact that gas molecules undergo much more rapid motion than in liquids, due to much longer free displacements between collisions. The farther the molecular displacements along the direction of the gradient, the faster the nuclear spins will lose memory of their immediate environment. This memory loss should be expected to enter the description of the decoherence process. Surprisingly, this simple aspect of free diffusion is still lacking a thorough experimental verification.

The NMR signal, $S(t)$, from an ensemble of spins initially located at $x(0)$ is given by the expectation value of the phase factor:

$$S(t) = \left\langle \exp\left[i \int_0^t \omega(t')dt'\right] \right\rangle, \tag{2}$$

where $\omega(t)$ describes the time-dependent resonance frequency offset (in the rotating frame). In the presence of a magnetic field gradient g, the resonance frequency is $\omega(t) = \gamma_n g x(t)$, where $x(t)$, the position of the nuclear spin after time t, is a random process. If we assume a Gaussian random process that is stationary in the wide sense, this expectation value takes the form [9]

$$\exp\left[i\gamma_n g \int_0^t \langle x(t')\rangle dt' - \gamma_n^2 g^2 \int_0^t \langle x(t')x(0)\rangle (t-t')dt'\right]. \tag{3}$$

The first term, $\exp[i\gamma_n g \int_0^t \langle x(t')\rangle dt']$, encodes the position in the phase of the spins [13] after undergoing

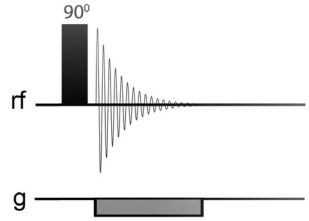

FIG. 1. Measurement of molecular self-diffusion in a constant field gradient. A 90° radio-frequency (rf) pulse tips the magnetization. This resulting nuclear induction signal is measured in a constant gradient of amplitude g. The time evolution of magnetization, as described by the textbook [10–12] expression (1), interrogates the molecular self-diffusion process.

displacement, but does not lead to decoherence unless the diffusion is not free. The second term describes signal decay, and consequently, affects linewidth. More complicated random processes may lead to higher-order terms, but we shall limit our discussion to the case where $x(t)$ is a wide-sense stationary Gaussian random process.

Over the time scale t of the NMR measurement, liquid phase molecules experience displacements that are much smaller than those in the gas phase. We may write this as $x(t) \approx x(0)$, for a liquid. This approximation, known as the Einstein-Fick limit, indicates that the position autocorrelation function can be approximated by the mean-square displacement

$$\langle x(t)x(0)\rangle \approx \langle x(t)x(t)\rangle = 2Dt, \tag{4}$$

where D is the self-diffusion coefficient. It is known from experiments that in liquids, this limit holds [10–12]. However, D_{liquid} and D_{gas} differ by 3 orders of magnitude, and it is unclear if this approximation also holds for gases. Away from the Einstein-Fick limit, contributions from ballistic transport become significant. We note that substitution of the limit (4) into the second term of Eq. (3) recovers the result (1) as a special case.

In this Letter, we show that Eq. (1) does not hold for gases based on the analysis of linewidth as a function of temperature (T). Because $D(T)$ increases with T, Eq. (1) predicts that linewidth should increase with T. We find that gases instead undergo line narrowing with temperature. It is unclear by cursory inspection of Eq. (1) how gases may differ from liquids, especially in light of the fact that the dependence of line broadening on the diffusion coefficient has been verified experimentally in several studies (see, for example, Refs. [11,14,15]). The key to establishing this distinction is a closer look at the temperature dependence of the line broadening mechanism, as explained below.

In the NMR experiment, nuclear spins are well isolated from the lattice and do not depolarize or randomize their phases when undergoing molecular collisions, in contrast to collisional broadening mechanisms in optics. Thus, the description of line broadening in such a "weak collision" regime reflects the histories of molecular displacements. The simplest way to account for this is through a position autocorrelation function. Suppose that the particle displacements are modeled using a generalized Langevin equation (GLE) with memory kernel:

$$M\dot{v} + \int_0^t \Gamma(t-t')v(t')dt' = \eta_f(t), \tag{5}$$

where M is the mass of the diffusing particle, $\Gamma(t)$ is a memory kernel, $v(t) = \dot{x}(t)$ is the particle velocity, $\dot{v}$ is its acceleration, and $\eta_f(t)$ is a stochastic force. The GLE has been validated experimentally for Brownian particles ($M \gg m$, where m is the mass of fluid particles); for example, in the studies of Refs. [16–19] M was 10^{10} times larger than m. So while the GLE was not designed to model self-diffusion processes, it can be invoked to model viscous drag effects via the memory kernel. In what follows, we shall set $M = 10^{10}m$, which is the only regime we are aware of where the GLE has been validated experimentally based on direct measurements of individual histories (namely, in Refs. [16–19]).

By the fluctuation-dissipation theorem, the stochastic force $\eta_f(t)$ describes colored noise, $\langle \eta_f(0)\eta_f(t)\rangle = kT\Gamma(t)$, where k is Boltzmann's constant. The time-correlation function $\langle x(t)x(0)\rangle$ is obtained from $\langle v(t)v(0)\rangle$ by integrating twice the velocity autocorrelation function

$$\langle v(t)v(0)\rangle = -\frac{d^2}{dt^2}\langle x(t)x(0)\rangle. \tag{6}$$

Projecting Eq. (5) with the operator $\langle v(0), \cdot\rangle$ yields the deterministic equation

$$M\langle v(0)\dot{v}(t)\rangle + \int_0^t \Gamma(t-t')\langle v(0)v(t')\rangle dt' = 0. \tag{7}$$

Integrating this velocity autocorrelation function once,

$$\nu(t) = \int_0^t \langle v(0)v(t')\rangle dt', \tag{8}$$

and using the equipartition theorem, $\langle v(0)v(0)\rangle = kT/M$, as the initial condition, we get

$$M\dot{\nu}(t) + \int_0^t \Gamma(t-t')\nu(t')dt' = kT. \tag{9}$$

For the memory kernel to describe the delayed response of the surrounding fluid, we choose the Ornstein-Uhlenbeck process:

$$\Gamma(t) = (\gamma^2/m)\exp(-\gamma t/m),$$

where γ is the friction coefficient proportional to the viscosity of the medium and m is the mass of molecules in the surrounding medium causing friction. Denoting $\zeta_{-,+} = (\gamma/2m)(1 \mp \sqrt{1-4m/M})$, we obtain the solution to Eq. (9):

$$\nu(t) = \frac{kT}{M}\left\{\frac{\gamma}{m\zeta_-\zeta_+} + \frac{1}{\zeta_+ - \zeta_-}\left[\left(1 - \frac{\gamma}{m\zeta_+}\right)e^{-\zeta_+ t} - \left(1 - \frac{\gamma}{m\zeta_-}\right)e^{-\zeta_- t}\right]\right\}. \tag{10}$$

From this we get the position autocorrelation function,

$$\langle x(t)x(0)\rangle = \frac{kT}{M(\zeta_+ - \zeta_-)}\left[\zeta_+^{-1}\left(1-\frac{\gamma}{m\zeta_+}\right)e^{-\zeta_+ t} - \zeta_-^{-1}\left(1-\frac{\gamma}{m\zeta_-}\right)e^{-\zeta_- t}\right]. \quad (11)$$

This result was also derived by Nørrelykke [20] using a different method. In the Einstein-Fick approximation, $x(0) \approx x(t)$, and this position autocorrelation function reduces to $2Dt$. Equation (11) generalizes $S(t)$ outside the Einstein-Fick limit. There are three distinct regimes: overdamped ($M > 4m$), critically damped ($4m = M$), and underdamped ($M < 4m$). Standard Brownian motion of large particles is strongly overdamped ($M \gg m$). The Einstein-Fick limit occurs when the ratio $\gamma t/m$ is sufficiently large to cause appreciable decay of the Ornstein-Uhlenbeck kernel. Using γ based on the Stokes's law and $t = 40\ \mu$s as the sampling time of the nuclear induction signal, we find that typical values of this ratio for liquids are $\gamma t/m \sim 1$, whereas for gases we have $\gamma t/m \ll 1$.

In the case of a gas, we may obtain the overall temperature by modeling γ using the Stokes's law, $\gamma = 3\pi\eta_v d$ (η_v, shear viscosity of the medium; d, sphere diameter), which holds in the limit of low Reynolds numbers and invoking Sutherland's formula [21] for η_v:

$$\eta_v = \frac{\mu_0(T_0 + C)(T/T_0)^{3/2}}{T + C} \sim \frac{T^{3/2}}{T + C}, \quad (12)$$

where C is Sutherland's constant for the gas, and μ_0 is the viscosity at temperature T_0. At low temperatures, $\eta_v \sim T^{3/2}$, whereas at high temperatures, $\eta_v \sim \sqrt{T}$. By substituting this into Eq. (12), we obtain at an expression for the envelope function of the signal decay for a gas which does not rely on the Einstein-Fick limit,

$$S(t) = \exp(-\gamma_n^2 g^2 \kappa t), \quad (13)$$

with

$$\kappa(T) = \frac{kT(-m\zeta_-^2\zeta_+ - m\zeta_-\zeta_+^2 + \zeta_-\gamma + \zeta_-\zeta_+\gamma + \zeta_+^2\gamma)}{mM\zeta_-^3\zeta_+^3}. \quad (14)$$

The linewidth Δf follows the power law

$$\Delta f \sim \begin{cases} T^{-7/2}, & T < C \\ T^{-1/2}, & T > C \end{cases}, \quad (15)$$

which predicts a temperature dependence that is opposite (i.e., line narrowing with increasing temperature) to that based on self-diffusion in the Einstein-Fick limit (1). An analogous expression in the case of liquids can be derived using a suitable model for the temperature dependence of the viscosity in a liquid. However, this will not be needed here, because we shall see that the linewidth is essentially independent of temperature.

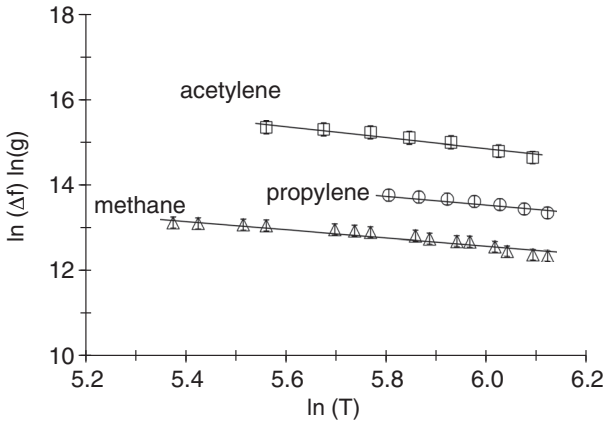

FIG. 2. Validation of the $T^{-1/2}$ law in the high-temperature regime ($T > C$) for gases. The values of ln T shown correspond to the temperature range $T = 180$–490 K. Three different gases were investigated: methane, acetylene, and propylene. The temperature dependence on linewidth (scaled to gradient strength) was found to be $\Delta f \propto T^{-0.47\pm0.04}$ (averaged over the three gases). Although different values of the applied gradient g are shown here to avoid overlapping of the curves (methane, $g = 0.15$ G/cm; acetylene, $g = 0.07$ G/cm; propylene, $g = 0.1$ G/cm), the scaled linewidth is independent of g.

Measurements of Δf were carried out as a function of T for three gases in the high temperature regime ($T > C$, as determined by the Sutherland's constant for each gas [22–25]). The results are shown in Fig. 2. The average exponent was found to be -0.47 ± 0.04, in agreement with the theoretically predicted value of $-1/2$ in Eq. (15). The low temperature regime ($T < C$) could not be investigated due to experimental limitations of our instrument. A temperature dependence of linewidth could not be detected within experimental error for liquids, as shown in Fig. 3, where we investigated nine different liquids over the range 180–450 K. We note that Sutherland's formula [and therefore, Eq. (13)] is applicable to gases only, so a lower limit on temperature for the liquids is imposed by the freezing points.

We now turn our attention to the gradient dependence of the line broadening, which, according to Eq. (13), should be proportional to g^2. In experiments, however, we found two regimes: in the limit of weak gradients, $\Delta f \propto g^2$, whereas for strong gradients, $\Delta f \propto g^1$ (see Figs. 4 and 5). The g^2 gradient dependence is predicted according to Eq. (13); however, the $\Delta f \propto g^1$ is not. Moreover, these two regimes apply to both liquids and gases, according to the results of Figs. 4 and 5. The emergence of the g^1 regime is likely due to the convolution of the line shape with the sample shape that arises under an applied gradient and forms the basis for frequency encoding in magnetic resonance imaging. The full signal equation integrated over the sample shape is

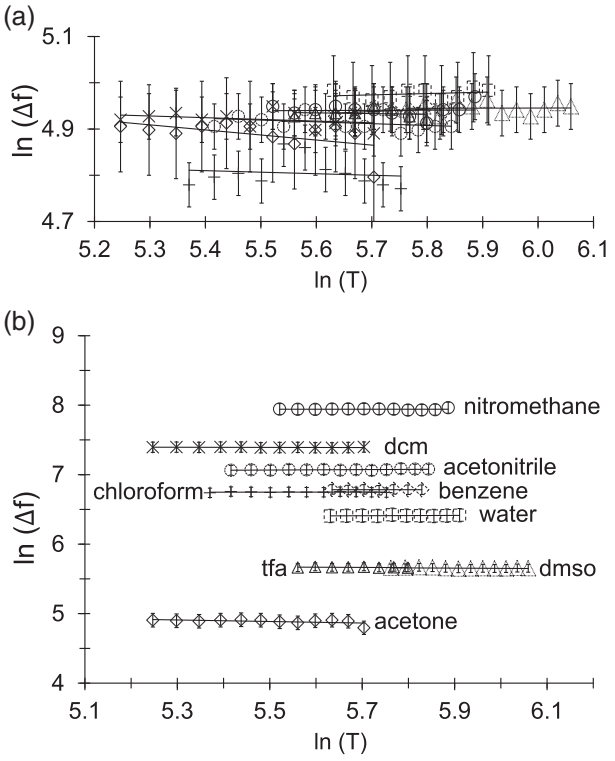

FIG. 3. Temperature dependence of linewidth (Δf) in liquids. Nine different liquids were investigated, as shown by the different symbols. The values of $\ln(T)$ shown span the temperature range $T = 180$–450 K. (a) For a fixed gradient strength of $g = 0.05$ G/cm, all linewidths were broadened by a similar amount, hence the overlap in the data. At fixed g, the linewidth did not exhibit any detectable dependence on temperature. (b) Increasing applied gradient strength did not alter the independence of linewidth on temperature. Applied gradient strengths were nitromethane (1 G/cm), dichloromethane (dcm, 0.5 G/cm), acetonitrile (0.4 G/cm), chloroform (0.3 G/cm), benzene (0.3 G/cm), water (0.2 G/cm), trifluoroacetic acid (tfa, 0.1 G/cm), dimethyl sulfoxide (dmso, 0.1 G/cm), acetone (0.05 G/cm). The symbol in (a) refers to the same liquid as in (b).

$$S(t) = \int \exp(i\gamma_n g x t)\exp(-\alpha g^2 t)\rho(x)dx, \qquad (16)$$

where $\rho(x)$ describes the spin density profile along the x direction (sample shape), $\exp(i\gamma_n g x t)$ is the frequency encoding, and $\exp(-\alpha g^2 t)$ is the line broadening according to Eq. (13). For the particular case where the sample shape $\rho(x)$ is Gaussian (a reasonable approximation for the sensitivity profile of a saddle coil, such as the one used in these experiments), the Fourier transform of Eq. (16) with respect to time is a convolution:

$$\tilde{S}(\omega) = \text{Gauss} \otimes \text{Lorentz} = \text{Voigt}, \qquad (17)$$

in which the Gaussian is $\sim\exp(-x^2/2\sigma^2)$, and the Lorentzian is $\sim\Gamma^2/(x^2+\Gamma^2)$. In terms of the full width at half maximum of the Gaussian ($f_G = 2\sigma\gamma g\sqrt{2\ln 2}$) and Lorentzian ($f_L = 2\Gamma = 2\alpha g^2$) profiles, the width of the Voigt profile can be expressed as $f_v \approx 0.5 f_L + \sqrt{0.2 f_L^2 + f_G^2}$. Thus, in the frequency encoding regime, where sample shape effects dominate, the line broadening behaves as g^1 regardless of whether Eqs. (1) or (13) are used to describe the diffusion effects. The frequency encoding regime is reached when the field of view FOV $= f_s/\gamma_n g$ (f_s, sampling rate; g, gradient amplitude), becomes comparable to the size of the rf-sensitive region (~1 cm in our experiments). Depending on the applied gradient strength, the experimental FOV ranges from 0.6 to 1460 cm. The FOV values corresponding to applied gradient (g) are indicated in the upper horizontal axes of Figs. 4 and 5, where the two regimes, g^1 and g^2, are indicated.

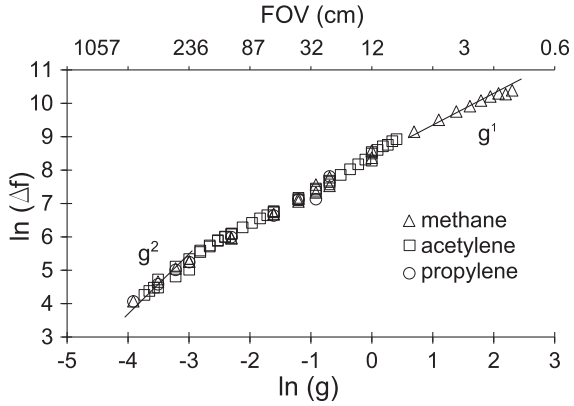

FIG. 4. Dependence of linewidth (Δf) on applied gradient strength (g) for gases. Three different gases were investigated. Two different regimes are found: in the limit of strong applied gradients, Δf scales as $g^{1.0\pm0.1}$ whereas for weak gradients Δf scales as $g^{1.8\pm0.2}$. All data were acquired at ambient temperature.

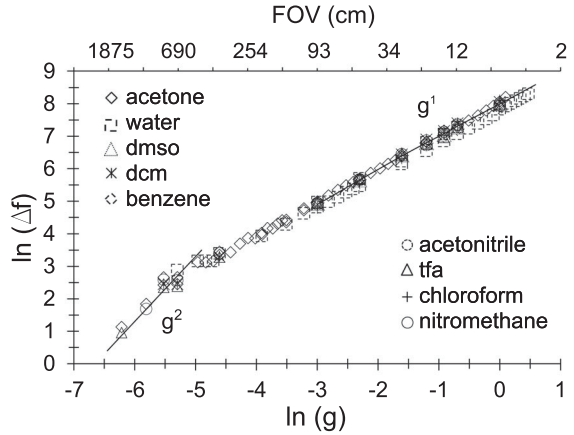

FIG. 5. Dependence of linewidth (Δf) on gradient strength (g) for liquids. Nine different liquids were investigated. Two different regimes are found: in the limit of strong applied gradients, Δf scales as $g^{1.1\pm0.1}$, whereas for weak gradients Δf scales as $g^{2.0\pm0.2}$. All data were acquired at ambient temperature.

We have presented a revised expression for line broadening Eq. (13) that not only takes into account the autocorrelation effects in the diffusion process, but also suggests that self-diffusion processes in the NMR experiment may be described using a stochastic GLE, at least, as far as its temperature dependence is concerned. The GLE approach (13) enables a convenient description of the memory effects arising from the viscous drag effects, which were essentially missing from the traditional description, Eq. (1). Such drag effects yielded the correct temperature dependence for gases and have been used in a recent publication to noninvasively map temperatures of gases during catalytic reactions [26]. The method could also be useful in the validation of heat-transfer models for gas-phase thermal exchange systems, which currently rely on numerical results from computational fluid dynamics models. Finally, we note that since the decay function Eq. (13) involves the first power of time instead of its third power Eq. (1), Eq. (13) could have implications for the design of dynamic decoupling schemes for coherent quantum control [27].

See Supplemental Material [22] for experimental methods, data analysis details, and sample data.

This work was partially funded by a Beckman Young Investigator Award and the National Science Foundation through Grant No. CHE-1153159.

*bouchard@chem.ucla.edu

[1] P. T. Callaghan, A. Coy, D. MacGowan, K. J. Packer, and F. O. Zelaya, Nature (London) **351**, 467 (1991).
[2] M. Hollewand and L. Gladden, J. Catal. **144**, 254 (1993).
[3] Y. Cohen, L. Avram, and L. Frish, Angew. Chem., Int. Ed. **44**, 520 (2005).
[4] D. Le Bihan, Nat. Rev. Neurosci. **4**, 469 (2003).
[5] N. Bloembergen, E. M. Purcell, and R. V. Pound, Phys. Rev. **73**, 679 (1948).
[6] E. L. Hahn, Phys. Rev. **80**, 580 (1950).
[7] H. Y. Carr and E. M. Purcell, Phys. Rev. **94**, 630 (1954).
[8] H. C. Torrey, Phys. Rev. **104**, 563 (1956).
[9] R. Kubo and K. Tomita, J. Phys. Soc. Jpn. **9**, 888 (1954).
[10] P. T. Callaghan, *Principles of Nuclear Magnetic Resonance Microscopy* (Clarendon Press, Oxford, 1991), Vol. 3.
[11] E. Stejskal and J. Tanner, J. Chem. Phys. **42**, 288 (1965).
[12] P. T. Callaghan, *Translational Dynamics and Magnetic Resonance: Principles of Pulsed Gradient Spin Echo NMR* (Oxford University Press, New York, 2011).
[13] D. G. Nishimura, *Principles of Magnetic Resonance Imaging* (Stanford University, Palo Alto, CA, 1996).
[14] D. Pines and C. P. Slichter, Phys. Rev. **100**, 1014 (1955).
[15] J. Stepišnik, Physica (Amsterdam) **183B**, 343 (1993).
[16] T. Li, S. Kheifets, D. Medellin, and M. G. Raizen, Science **328**, 1673 (2010).
[17] R. Huang, I. Chavez, K. M. Taute, B. Lukić, S. Jeney, M. G. Raizen, and E.-L. Florin, Nat. Phys. **7**, 576 (2011).
[18] T. Franosch, M. Grimm, M. Belushkin, F. M. Mor, G. Foffi, L. Forró, and S. Jeney, Nature (London) **478**, 85 (2011).
[19] S. Kheifets, A. Simha, K. Melin, T. Li, and M. G. Raizen, Science **343**, 1493 (2014).
[20] S. F. Nørrelykke and H. Flyvbjerg, Phys. Rev. E **83**, 041103 (2011).
[21] S. Chapman and T. G. Cowling, *The Mathematical Theory of Non-Uniform Gases: an Account of the Kinetic Theory of Viscosity, Thermal Conduction and Diffusion in Gases* (Cambridge University Press, Cambridge, England, 1970).
[22] See Supplemental Material at http://link.aps.org/supplemental/10.1103/PhysRevLett.114.197601, for experimental methods, data analysis details, and sample data, which includes Refs. [21,23–25].
[23] C. Ammann, P. Meier, and A. Merbach, J. Magn. Reson. **46**, 319 (1982).
[24] W. Haynes, *CRC Handbook of Chemistry and Physics* (CRC Press, Boca Raton, 2014–2015).
[25] W. Sutherland, Philos. Mag. **17**, 320 (1909).
[26] N. N. Jarenwattananon, S. Glöggler, T. Otto, A. Melkonian, W. Morris, S. R. Burt, O. M. Yaghi, and L.-S. Bouchard, Nature (London) **502**, 537 (2013).
[27] G. Uhrig, Phys. Rev. Lett. **98**, 100504 (2007).